Author's Accepted Manuscript

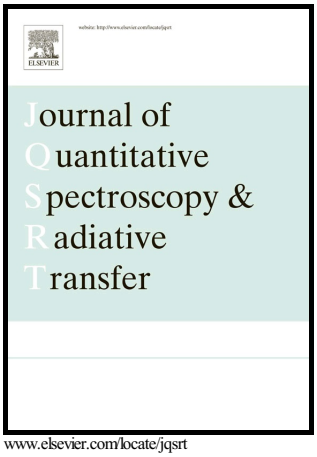

www.elsevier.com/locate/jqsrt

Optics of water microdroplets with soot inclusions: Exact versus approximate results

Li Liu, Michael I. Mishchenko

PII: S0022-4073(15)30135-7
DOI: http://dx.doi.org/10.1016/j.jqsrt.2015.12.025
Reference: JQSRT5170

To appear in: *Journal of Quantitative Spectroscopy and Radiative Transfer*

Received date: 16 September 2015
Revised date: 24 December 2015
Accepted date: 24 December 2015

Cite this article as: Li Liu and Michael I. Mishchenko, Optics of wate microdroplets with soot inclusions: Exact versus approximate results, *Journal o Quantitative Spectroscopy and Radiative Transfer* http://dx.doi.org/10.1016/j.jqsrt.2015.12.025

Note

Optics of water microdroplets with soot inclusions: exact versus approximate results

Li Liu[a,b,*], Michael I. Mishchenko[b]

[a]*Columbia University, 2880 Broadway, New York, NY 10025, USA*
[b]*NASA Goddard Institute for Space Studies, 2880 Broadway, New York, NY 10025, USA*

[*]Corresponding author. Fax: +1 212 678 5622.
E-mail address: ll360360@gmail.com (L. Liu).

Abstract

We use the recently generalized version of the multi-sphere superposition *T*-matrix method (STMM) to compute the scattering and absorption properties of microscopic water droplets contaminated by black carbon. The soot material is assumed to be randomly distributed throughout the droplet interior in the form of numerous small spherical inclusions. Our numerically-exact STMM results are compared with approximate ones obtained using the Maxwell-Garnett effective-medium approximation (MGA) and the Monte Carlo ray-tracing approximation (MCRTA). We show that the popular MGA can be used to calculate the droplet optical cross sections, single-scattering albedo, and asymmetry parameter provided that the soot inclusions are quasi-uniformly distributed throughout the droplet interior, but can fail in computations of the elements of the scattering matrix depending on the volume fraction of soot inclusions. The integral radiative characteristics computed with the MCRTA can deviate more significantly from their exact STMM counterparts, while accurate MCRTA computations of the phase function require droplet size parameters substantially exceeding 60.

Keywords:
Cloud droplets
Soot inclusions
Electromagnetic scattering
Superposition *T*-matrix method
Ray-tracing method
Effective-medium approximation

1. Introduction

It is widely recognized that black carbon (or soot) aerosols can act as cloud condensation nuclei and serve as cloud-droplet pollutants [1–3]. Internal contamination of cloud droplets by soot may cause substantial changes in the optical and radiative properties of liquid-water clouds (see, e.g., [4–6] and references therein). Numerically-accurate calculations of electromagnetic scattering and absorption by cloud droplets with multiple absorbing inclusions have represented a challenging problem because direct computer solutions of the macroscopic Maxwell equations for such complex and relatively large particles have been impracticable until quite recently [7,8]. As a consequence, various approximate approaches have had to be used. For example, calculations of the atmospheric energy budget have relied heavily on heuristic effective-medium approximations (EMAs) [5,6,9,10] as a means of taking into account the optical effects of internal mixing. The EMAs are based on modeling complex heterogeneous particles as being homogeneous and having a refractive index computed with one of the phenomenological mixing rules such as the Lorentz–Lorenz, Bruggeman, and Maxwell-Garnett mixing formulas [9]. Another approximate approach frequently used to calculate single-scattering properties of large cloud, snow, and soil particles containing numerous inclusions is the Monte Carlo ray-tracing approximation (MCRTA) which treats the inclusions as point-like scatterers described by the Lorenz–Mie theory (e.g., [11–15]). However, the accuracy and range of applicability of such approximate methodologies have been poorly known.

The concept of a T matrix was introduced by Waterman in 1971 [16] and has been widely used in studies of electromagnetic scattering and absorption by morphologically complex particles [17–24]. The most recent version of the multi-sphere superposition T-matrix method (STMM) developed by Mackowski [25] has extended the formulation to arbitrary configurations of spherical domains wherein any of the spheres can be located at points that are either internal or external to the other spheres. As a result, the method became applicable to the case of internal mixing (according to the definition in [26]). Unlike the approximate methodologies, the STMM is a direct computer solver of the frequency-domain macroscopic Maxwell equations and renders solutions that are both numerically exact and highly efficient. Furthermore, the STMM program can now be run on distributed-memory computer clusters as well as on serial platforms. The parallel-computing option enables accurate calculations of absorption and scattering characteristics of internal mixtures containing tens of thousands of inclusions [27–29] as well as exquisite ensemble averaging [30]. Quite expectedly, however, the numerical effort becomes prohibitive and the number of inclusions has to be reduced when the host size parameter increases and approaches ~100.

Given the availability of this improved version of the STMM methodology, the main objective of this Note is to model typical effects of multiple quasi-randomly distributed absorptive inclusions on the scattering and absorption properties of microscopic spherical water droplets. We then compare the numerically-exact STMM results with those computed with the Maxwell-Garnett EMA and the MCRTA in order to evaluate and quantify the corresponding errors in the integral radiometric characteristics and scattering-matrix elements. We expect that doing so will provide guidance to researchers in deciding whether to use either approximate approach in specific applications depending on the acceptable level of numerical uncertainty.

2. Numerical results and discussion

A recent study has revealed that for the same cumulative amount of an absorptive foreign material, the absorption is maximized when the material is distributed quasi-uniformly

throughout the droplet interior in the form of numerous small inclusions [31]. Another reason to focus on this model of heterogeneous water droplets is that it appears to be the only internal-mixing scenario that can potentially make applicable the EMA concept and the MCRTA [27–32].

To model this type of heterogeneity, we place an increasing number (N = 10, 25, 50, 100, 200, 300, 400, 500, and 600) of spherical soot inclusions quasi-randomly inside a spherical host water droplet, as illustrated in Fig. 1. The positions of the soot inclusion cannot be completely random since these particles are not allowed to overlap. However, assigning the inclusion coordinates using a random-number generator and then averaging over the uniform orientation distribution of the resulting heterogeneous droplet yields in effect a scattering object with a random and statistically uniform distribution of inclusions. All soot inclusions are assumed to be identical, with their size parameter fixed at $k_1 r = 1$, where $k_1 = 2\pi/\lambda$ is the wave number in the infinite nonabsorbing medium surrounding the droplet and r = 0.1 μm is radius of the inclusions. The wavelength λ is fixed at $\pi/5$ μm ≈ 0.6283 μm, thereby implying that $k_1 = 10$. The soot refractive index, 1.95+0.79i, is chosen according to the recommendation in [33], while the host refractive index, 1.33, is representative of liquid water at visible and near-infrared wavelengths.

Note that the size spectrum of black-carbon aerosols serving as cloud condensation nuclei is wide and sometimes can span several orders of magnitude [34,35]. The inclusion sizes affect the overall light scattering and absorption of heterogeneous particles [13,28,29]. Ideally one would need to assume that these embedded particulates are polydisperse and randomly distributed inside a water droplet. However, instead of estimating the actual radiative impact by soot-contaminated cloud droplets, the main goal of this study is to examine the applicability of approximate theories such as the Maxwell-Garnett EMA and the MCRTA in computations of scattering and absorption characteristics of heterogeneous water–soot mixtures by comparing their outputs with numerically-exact STMM results. Moreover, the black-carbon radius of 0.1 μm is a representative value consistent with both models and observations [36,37].

The integral radiometric characteristics typically used to describe the single-scattering and absorption properties of atmospheric particulates include the ensemble-averaged extinction, $C_{\rm ext}$, scattering, $C_{\rm sca}$, and absorption, $C_{\rm abs} = C_{\rm ext} - C_{\rm sca}$, cross sections; the single-scattering albedo $\varpi = C_{\rm sca}/C_{\rm ext}$; and the asymmetry parameter g [19,38]. The angular distribution and the polarization state of the singly scattered light are nominally described in terms of the normalized Stokes scattering matrix

$$\tilde{\mathbf{F}}(\Theta) = \begin{bmatrix} a_1(\Theta) & b_1(\Theta) & 0 & 0 \\ b_1(\Theta) & a_2(\Theta) & 0 & 0 \\ 0 & 0 & a_3(\Theta) & b_2(\Theta) \\ 0 & 0 & -b_2(\Theta) & a_4(\Theta) \end{bmatrix}, \tag{1}$$

where $\Theta \in [0°, 180°]$ is the scattering angle (i.e., the angle between the incidence and scattering directions) [19,38]. Note that the specific block-diagonal structure of the scattering matrix (1) has been confirmed by all the STMM results discussed below. The (1, 1) element of the scattering matrix is the conventional phase function normalized according to

$$\frac{1}{2}\int_0^\pi {\rm d}\Theta \sin\Theta\, a_1(\Theta) = 1, \tag{2}$$

while the asymmetry parameter is defined according to

$$g = \frac{1}{2}\int_0^{\pi} \mathrm{d}\Theta \sin\Theta \cos\Theta \; a_1(\Theta). \tag{3}$$

In the case of heterogeneous water droplets, the orientation-averaged values of the above optical characteristics are calculated by running the STMM program developed in [25]. To suppress the scattering resonances typical of monodisperse objects [19,38], all scattering and absorption characteristics are further averaged over three discrete host size parameters, k_1R = 59, 60, and 61. These size-parameter values correspond to droplet radii R = 5.9, 6, and 6.1 μm which lie in the range of observed effective radii of cloud droplets in the terrestrial atmosphere, perhaps somewhat on the smaller side [39,40]. The quasi-random positions of the soot inclusions are generated separately for each host size parameter. Note that as the number of the inclusions increases from 10 to 600 inside a 6-μm droplet, the corresponding volume fraction of the soot material grows from 4.63×10^{-5} to 2.78×10^{-3}.

The solid curves in Fig. 2 show the orientation- and size-averaged elements of the Stokes scattering matrix as functions of the scattering angle for N = 100 and 600. For comparison, the dotted curves depict the corresponding Lorenz–Mie results for homogeneous droplets with refractive indices calculated using the Maxwell-Garnett approximation (MGA) for the respective volume fractions of soot in the k_1R = 60 droplet. In this case the water droplets are assumed to be polydisperse and characterized by a very narrow power law size distribution [19,41] with an effective size parameter of 60 and an effective variance of 0.001.

The STMM results in Fig. 2 show that as the number of absorbing inclusions increases, the phase functions of the soot-contaminated droplets become progressively smooth and shallow at side-scattering angles, while the characteristic rainbow and glory features weaken. Furthermore, the deviation of the ratio $a_2(\Theta)/a_1(\Theta)$ from unity increases and exhibits strong backscattering depolarization qualitatively attributable to the growing contribution of "multiple internal scattering".

Although the phase functions rendered by the MGA are qualitatively similar to their STMM counterparts, substantial quantitative differences are quite obvious. For example, at the exact backscattering direction, the $a_1(180°)$ difference between the STMM and MGA results exceeds a factor of three in the case of the droplets with 100 soot inclusions (see the left-hand panel of Fig. 3). The corresponding phase-function differences at side-scattering angles for N = 600 exceed a factor of two. The differences in the ratios $a_j(\Theta)/a_1(\Theta)$ and $\pm b_j(\Theta)/a_1(\Theta)$ can partly be attributed to the use of different size distributions in the STMM and MGA computations, but in some cases they obviously have a component caused by the very use of an approximate scattering methodology. Most importantly, whenever the MGA is applied to a spherical host it reproduces the two fundamental Lorenz–Mie identities,

$$\frac{a_2(\Theta)}{a_1(\Theta)} \equiv 1 \text{ and } \frac{a_3(\Theta)}{a_4(\Theta)} \equiv 1. \tag{4}$$

However, Fig. 2 reveals a substantial violation of the first identity by the numerically-exact STMM results. The violation of the second identity, as illustrated by the right-hand panel of Fig. 3, is equally pronounced. These results confirm once again an essential limitedness of the concept of effective refractive index.

Fig. 4 compares the phase functions computed for the water microdroplets with an increasing number of soot inclusions using the STMM and the MCRTA. The latter is a simple

and efficient heuristic method combining ray-optics and radiative-transfer concepts. It permits the treatment of light scattering and absorption by arbitrarily shaped host particles containing small, randomly positioned, widely separated inclusions and is expected to be applicable to host particles with sizes much greater than the wavelength of the incident radiation. In an *ad hoc* fashion, the ray-tracing program takes care of individual reflection and refraction events at the outer boundary of the host particle, while the Monte Carlo procedure essentially simulates the summation of the so-called ladder diagrams appearing in the microphysical theory of radiative transfer [38,42]. This model is detailed in [11,12,43–45] and is implemented in the form of a computer program publicly available at http://tools.tropos.de. This specific program is based on the so-called scalar approximation of radiative transfer [42] and hence can be used to compute only the $(1, 1)$ element of the scattering matrix (i.e., the phase function).

It is obvious from Fig. 4 that the MCRTA is unable to reproduce the strong backscattering enhancement traditionally called the glory. Furthermore, the sharpness and magnitude of the primary and secondary rainbows rendered by the MCRTA are grossly overestimated. The side-scattering differences between the STMM and MCRTA phase functions are also quite pronounced. One can think of several potential causes of these side- and backscattering differences, including the inadequacy of the ray-tracing concepts of reflections and refractions and the failure of the radiative-transfer concept of ladder sequences of widely separated particles [38,42]. The numerical comparisons of ray-tracing and Lorenz–Mie results in [19,41] and of radiative-transfer and STMM results in [46] suggest that the failure of the ray-tracing concepts is likely to be the more significant factor.

Fig. 5 further quantifies the accuracy of the MGA and MCRTA as a function of the number of inclusions N. Note that the extinction cross section computed by the MCRTA for a particle much larger than the wavelength is identically equal to twice the area of the particle's projection on the plane normal to the incidence direction, the diffraction on and the geometric interception of the "incident rays" by the particle's projection being equal contributors. We define the relative errors of the approximate results, in percent, as $(C_{\rm approx}/C_{\rm STMM} - 1)\times 100\%$, where C represents any parameter of interest. The relative MGA errors as a function of the number of soot inclusions fall within the ranges [–4.44%, 7.82%], [–0.98%, 0.03%], and [0.10%, 2.75%] for the absorption cross section, single-scattering albedo, and asymmetry parameter, respectively. The corresponding MCRTA ranges are [–31.43%, –18.16%], [0.10%, 2.77%], and [2.49%, 2.75%]. The errors of both sets of approximate results usually grow with the number of soot inclusions. The notable exception is the MCRTA asymmetry parameter whose significant deviation from its STMM counterpart is essentially N-independent.

The reader should recall that the soot volume fraction at $N = 600$ is 2.78×10^{-3}. The real degree of soot contamination in terrestrial water clouds is unlikely to reach such high values [4,47–49]. Therefore, we conclude that the popular Maxwell-Garnett mixing rule can be safely used to calculate the optical cross sections, single-scattering albedo, and symmetry parameter for the quasi-uniform internal mixing scenario. Although the average performance of the MCRTA is not as good as that of the MGA, its accuracy can be expected to improve as the host water droplets become larger.

3. Concluding remarks

Our numerically exact single-scattering STMM results show that the presence of soot in water microdroplets can have a noticeable effect on their extinction, scattering, and absorption cross sections, single scattering albedo, asymmetry parameter, and, especially, elements of the

scattering matrix. The significant linear depolarization evident from the $a_2(\Theta)/a_1(\Theta)$ ratio is the prime manifestation of the morphological complexity of soot-contaminated droplets despite their perfectly spherical outer boundaries. Our results indicate that the Maxwell-Garnett effective-medium approximation can be safely used to calculate the integral radiative characteristics of soot-contaminated droplets but, depending on the actual volume fraction of soot, can fail in computations of the elements of the scattering matrix. Droplet size parameters ~60 are not sufficiently large for the MCRTA to yield adequately accurate phase functions. One can expect, however, that as the droplet size parameter increases the accuracy of the MCRTA can become significantly better. In general, our study testifies against indiscriminate use of the approximate methods in remote-sensing applications dealing with soot-contaminated cloud droplets.

Besides the MGA, another popular EMA is the so-called Bruggeman mixing rule [9,50]. If the volume fraction of the inclusions is substantial then the predictions of the two mixing rules can, in principle, differ. However, in the case of volume fractions as small as those considered in this Note both mixing rules yield nearly identical results despite the large refractive-index mismatch between liquid water and soot. Therefore, all conclusions reached above for the MGA are also valid for the Bruggeman mixing rule.

On a final note, we hope that our methodology of obtaining physical insight into the validity of the two approximate methods will find applications in light-scattering parameterization development. A good example would be the analysis of such important aspects of characterizing ambient aerosols as the interconnection between the effective refractive index and the effective particle mass density as well as the consistency of mixing rules used to calculate these two parameters of a multicomponent mixture via the index–density relationship [51].

Acknowledgments

We appreciate numerous useful discussions with Zhanna Dlugach, Michael Kahnert, and Daniel Mackowski. This research was funded by the NASA Remote Sensing Theory Project managed by Lucia Tsaoussi. All numerical results reported in this paper were obtained with the "Discover" supercomputer at the NASA Center for Climate Simulation.

References

[1] Dusek U, Reischl GP, Hitzenberger R. CCN activation of pure and coated carbon black particles. Environ Sci Technol 2006;40:1223–30.

[2] Kuwata M, Kondo Y, Takegawa N. Critical condensed mass for activation of black carbon as cloud condensation nuclei in Tokyo. J Geophy Res 2009;114:D20202.

[3] Spracklen DV, Carslaw KS, Pöschl U, Rap A, Forster PM. Global cloud condensation nuclei influenced by carbonaceous combustion aerosol. Atmos Chem Phys 2011;11:9067–87.

[4] Chýlek P, Lesins GB, Videen G, Wong JGD, Pinnick RG, Ngo D, Klett JD. Black carbon and absorption of solar radiation by clouds. J Geophys Res 1996;101:23365–71.

[5] Li J, Mlawer E, Chýlek P. Parameterization of cloud optical properties for semidirect radiative forcing. J Geophys Res 2011;116:D23212.

[6] Wang Z, Zhang H, Li J, Jing X, Lu P. Radiative forcing and climate response due to the presence of black carbon in cloud droplets. J Geophys Res 2013;118:3662–75.

[7] Mishchenko MI, Wiscombe WJ, Hovenier JW, Travis LD. Overview of scattering by nonspherical particles. In Mishchenko MI, Hovenier JW, Travis LD, editors. Light scattering by nonspherical particles: theory, measurements, and applications. San Diego: Academic Press; 2000. p. 29–60.

[8] Kahnert FM. Numerical methods in electromagnetic scattering theory. J Quant Spectrosc Radiat Transfer 2003;79–80:775–84.

[9] Chýlek P, Videen G, Geldart DJW, Dobbie JS, Tso HCW. Effective medium approximations for heterogeneous particles. In Mishchenko MI, Hovenier JW, Travis LD, editors. Light scattering by nonspherical particles: theory, measurements, and applications. San Diego: Academic Press; 2000. p. 273–308.

[10] Erlick C. Effective refractive indices of water and sulfate drops containing absorbing inclusions. J Atmos Sci 2006;63:754–63.

[11] Macke A, Mishchenko MI, Cairns B. The influence of inclusions on light scattering by large ice particles. J Geophys Res 1996;101:23311–16.

[12] Macke A. Monte Carlo calculations of light scattering by large particles with multiple internal inclusions. In Mishchenko MI, Hovenier JW, Travis LD, editors. Light scattering by nonspherical particles: theory, measurements, and applications. San Diego: Academic Press; 2000. p. 309–22.

[13] Liu L, Mishchenko MI, Menon S, Macke A, and Lacis A. The effect of black carbon on scattering and absorption of solar radiation by cloud droplets. J Quant Spectrosc Radiat Transfer 2002;74:195–204.

[14] C.-Labonnote L, Brogniez G, Buriez J-C, Doutriaux-Boucher M, Gayet J-F, Macke A. Polarized light scattering by inhomogeneous hexagonal monocrystals. Validation with ADEOS-POLDER measurements. J Geophys Res 2001;106:12139–53.

[15] Xie Y, Yang P, Kattawar GW, Minnis P, Hu YX. Effect of the inhomogeneity of ice crystals on retrieving ice cloud optical thickness and effective particle size. J Geophys Res 2009;114:D11203.

[16] Waterman PC. Symmetry, unitarity, and geometry in electromagnetic scattering. Phys Rev D 1971;3:825–39.

[17] Tsang L, Kong JA, Shin RT. Theory of microwave remote sensing. New York: Wiley; 1985.

[18] Doicu A, Eremin YuA, Wriedt T. Acoustic and electromagnetic scattering analysis using discrete sources. San Diego: Academic Press; 2000.

[19] Mishchenko MI, Travis LD, Lacis AA. Scattering, absorption, and emission of light by small particles. Cambridge: Cambridge University Press; 2002.

[20] Doicu A, Wriedt T, Eremin YuA. Light scattering by systems of particles. Null-field method with discrete sources: theory and programs. Berlin: Springer; 2006.

[21] Borghese F, Denti P, Saija R. Scattering from model nonspherical particles. Theory and applications to environmental physics. Berlin: Springer; 2007.

[22] Mishchenko MI, Videen G, Babenko VA, Khlebtsov NG, Wriedt T. *T*-matrix theory of electromagnetic scattering by particles and its applications: a comprehensive reference database. J Quant Spectrosc Radiat Transf 2004;88:357–406.

[23] Mishchenko MI, Zakharova NT, Khlebtsov NG, Wriedt T, Videen G. Comprehensive thematic *T*-matrix reference database: a 2013–2014 update. J Quant Spectrosc Radiat Transf 2014;146:349–54.

[24] Kahnert M. Numerical solutions of the macroscopic Maxwell equations for scattering by non-spherical particles: a tutorial review. J Quant Spectrosc Radiat Transf 2016 (in press).

[25] Mackowski DW. A general superposition solution for electromagnetic scattering by multiple spherical domains of optically active media. J Quant Spectrosc Radiat Transf 2014;133:264–70.

[26] Mishchenko MI, Liu L, Travis LD, Lacis AA. Scattering and radiative properties of semi-external versus external mixtures of different aerosol types. J Quant Spectrosc Radiat Transf 2004;88:139–47.

[27] Mishchenko MI, Dlugach ZM, Zakharova NT. Direct demonstration of the concept of unrestricted effective-medium approximation. Opt Lett 2014;39:3935–8.

[28] Mishchenko MI, Dlugach JM, Yurkin MA, Bi L, Cairns B, Liu L, Panetta RL, Travis LD, Yang P, Zakharova NT. First-principle modeling of electromagnetic scattering by discrete and discretely heterogeneous random media. Phys Rep 2016 (submitted).

[29] Mishchenko MI, Dlugach JM, Liu L. Applicability of the effective-medium approximation to heterogeneous aerosol particles. J Quant Spectrosc Radiat Transfer, in press, 2016.

[30] Kahnert M. Modelling radiometric properties of inhomogeneous mineral dust particles: applicability and limitations of effective medium theories. J Quant Spectrosc Radiat Transf 2015;152:16–27.

[31] Mishchenko MI, Liu L, Cairns B, Mackowski DW. Optics of water cloud droplets mixed with black-carbon aerosols. Opt Lett 2014;39:2607–10.

[32] Liu C, Panetta RL, Yang P. Inhomogeneity structure and the applicability of effective medium approximations in calculating light scattering by inhomogeneous particles. J Quant Spectrosc Radiat Transf 2014;146:331–48.

[33] Bond TC, Bergstrom RW. Light absorption by carbonaceous particles: an investigative review. Aerosol Sci and Tech 2006;40:27–67.

[34] Schroder JC, Hanna SJ, Modini RL, Corrigan AL, Kreidenwies SM, Macdonald AM, et al. Size-resolved observations of refractory black carbon particles in cloud droplets at a marine boundary layer site. Atmos Chem Phys 2015;15:1367–83.

[35] Taylor JW, Allan JD, Allen G, Coe H, Williams PI, Flynn MJ, et al. Size-dependent wet removal of black carbon in Canadian biomass burning plumes. Atmos Chem Phys 2014;14:13755–71.

[36] Koch D, Schulz M, Kinne S, McNaughton C, Spackman JR, Balkanski Y, et al. Evaluation of black carbon estimations in global aerosol models. Atmos Chem Phys 2009;9:9001–26.

[37] Adachi K, Zaizen Y, Kajino M, Igarashi Y. Mixing state of regionally transported soot particles and the coating effect on their size and shape at a mountain site in Japan. J Geophys Res Atmos 2014;119:5386–96.

[38] Mishchenko MI. Electromagnetic scattering by particles and particle groups: an introduction. Cambridge, UK: Cambridge University Press; 2014.

[39] Miles NL, Verlinde J, Clothiaux EE. Cloud size distribution in low-level stratiform clouds. J Atmos Sci 2000;57:295–311.

[40] Hudson JG, Yum SS. Maritime-continental drizzle contrasts in small cumuli. J Atmos Sci 2001;58:915–26.

[41] Hansen JE, Travis LD. Light scattering in planetary atmospheres. Space Sci Rev 1974;16:527–610.

[42] Mishchenko MI, Travis LD, Lacis AA. Multiple scattering of light by particles: radiative transfer and coherent backscattering. Cambridge, UK: Cambridge University Press; 2006.

[43] Macke A. Scattering of light by polyhedral ice crystals. Appl Opt 1993;32:2780–88.

[44] Macke A, Mueller J, Raschke E. Single scattering properties of atmospheric ice crystals. J Atmos Sci 1996;53:2813–25.

[45] Mishchenko MI, Macke A. Asymmetry parameters of the phase function for isolated and densely packed spherical particles with multiple internal inclusions in the geometric optics limit. J Quant Spectrosc Radiat Transf 1997;57:767–94.

[46] Muinonen K, Mishchenko MI, Dlugach JM, Zubko E, Penttilä A, Videen G. Coherent backscattering verified numerically for a finite volume of spherical particles. Astrophys J 2012;760:118.

[47] Chýlek P, Banic CM, Johnson B, Damiano PA, Isaac GA, Leaitch WR, Liu PSK, Boudala FS, Winter B, Ngo F D. Black carbon: atmospheric concentrations and cloud water content measurements over southern Nova Scotia. J Geophys Res 1996;101:29105–10.

[48] Hitzenberger R, Berner A, Giebl H, Drobesch K, Kasper-Giebl A, Loeflund M, Urban H, Puxbaum H. Black carbon (BC) in alpine aerosols and cloud water – concentrations and scavenging efficiencies. Atmos Environ 2001;35:5135–41.

[49] Twohy CH, Clarke AD, Warren SG, Radke LF, Charlson RJ. Light-absorbing material extracted from cloud droplets and its effect on cloud albedo. J Geophys Res 1989;94:8623–31.

[50] Sihvola A. Electromagnetic mixing formulae and applications. London: IEE Press; 1999.

[51] Liu Y, Daum PH. Relationship of refractive index to mass density and self-consistency of mixing rules for multicomponent mixtures like ambient aerosols. J Aerosol Sci 2008;39:974–986.

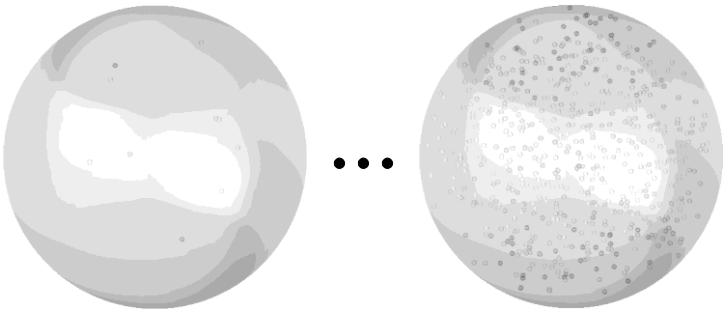

Fig. 1. Spherical water microdroplets populated with an increasing number N of spherical soot inclusions ranging from $N = 10$ to $N = 600$.

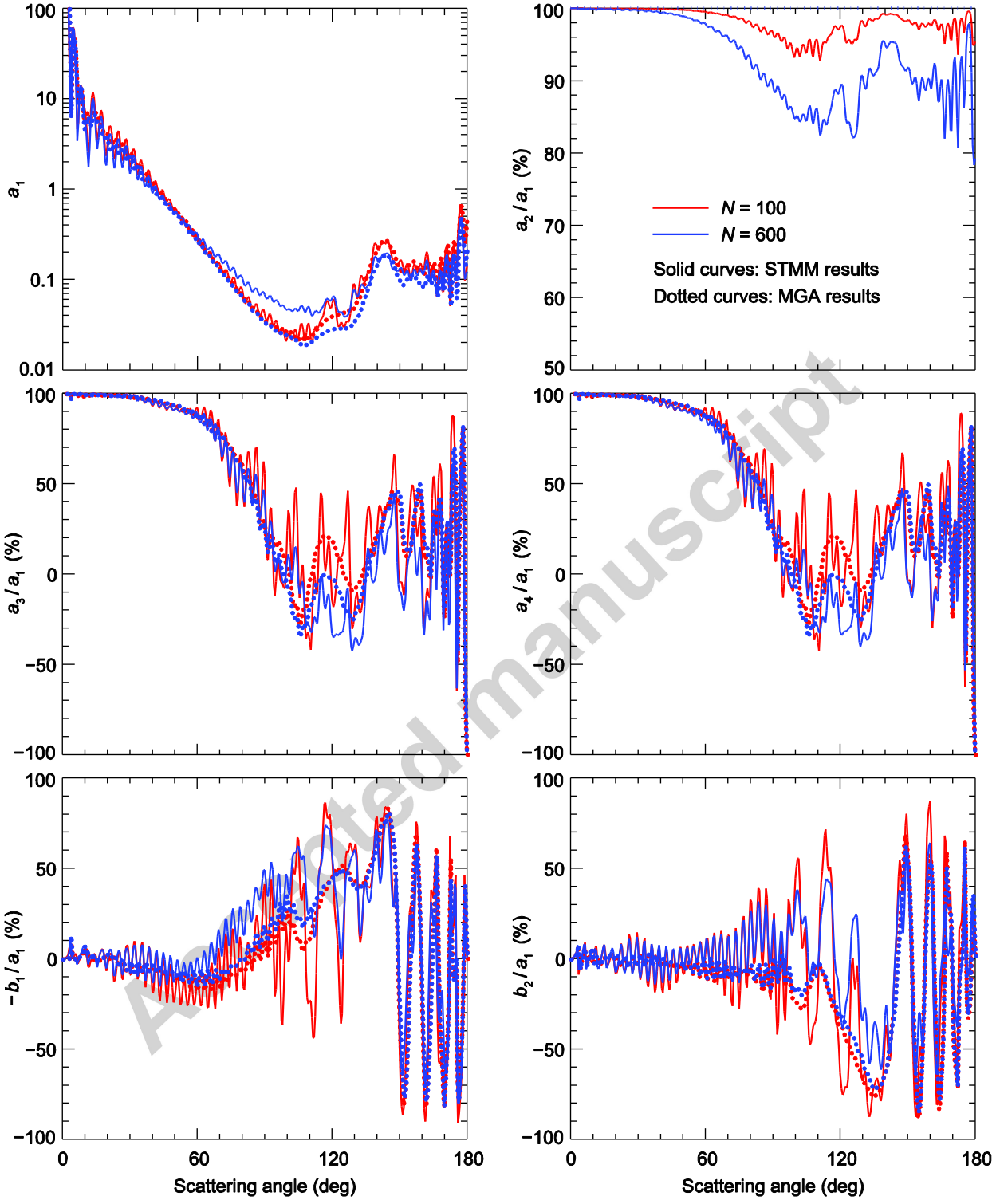

Fig. 2. Ensemble-averaged elements of the Stokes scattering matrix for soot-contaminated water microdroplets.

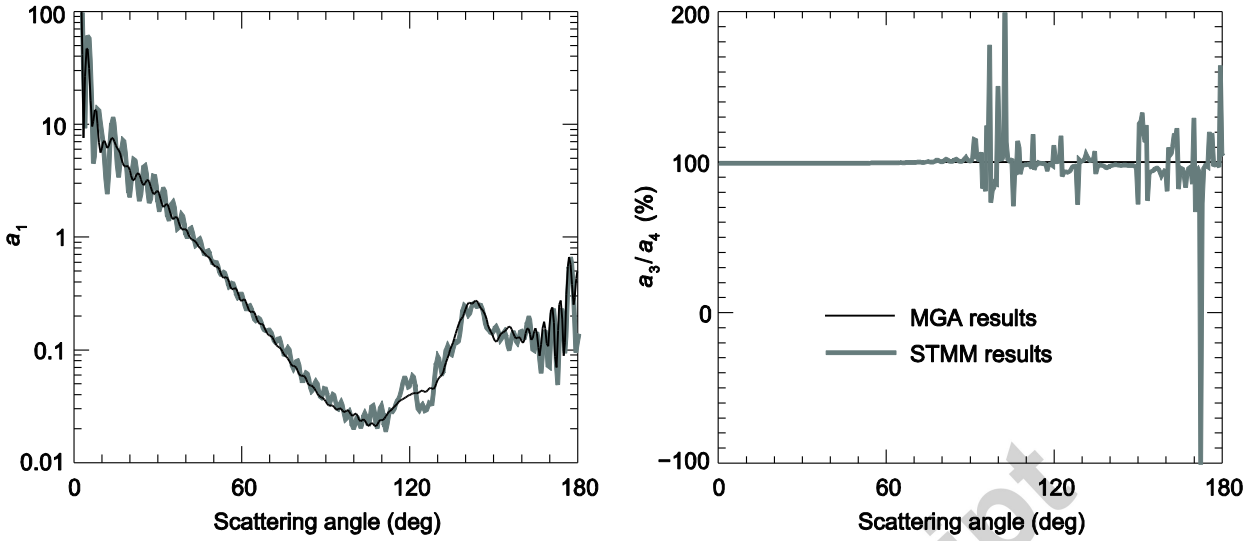

Fig. 3. The phase function and the ratio $a_3(\Theta)/a_4(\Theta)$ for water droplets with 100 soot inclusions.

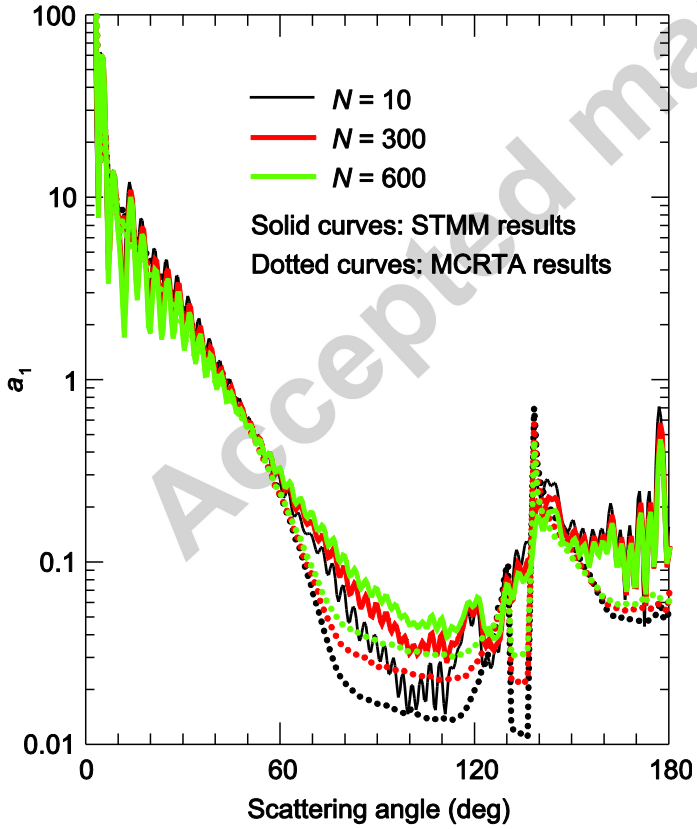

Fig. 4. Comparison of the STMM phase functions (solid curves) and their MCRTA counterparts.

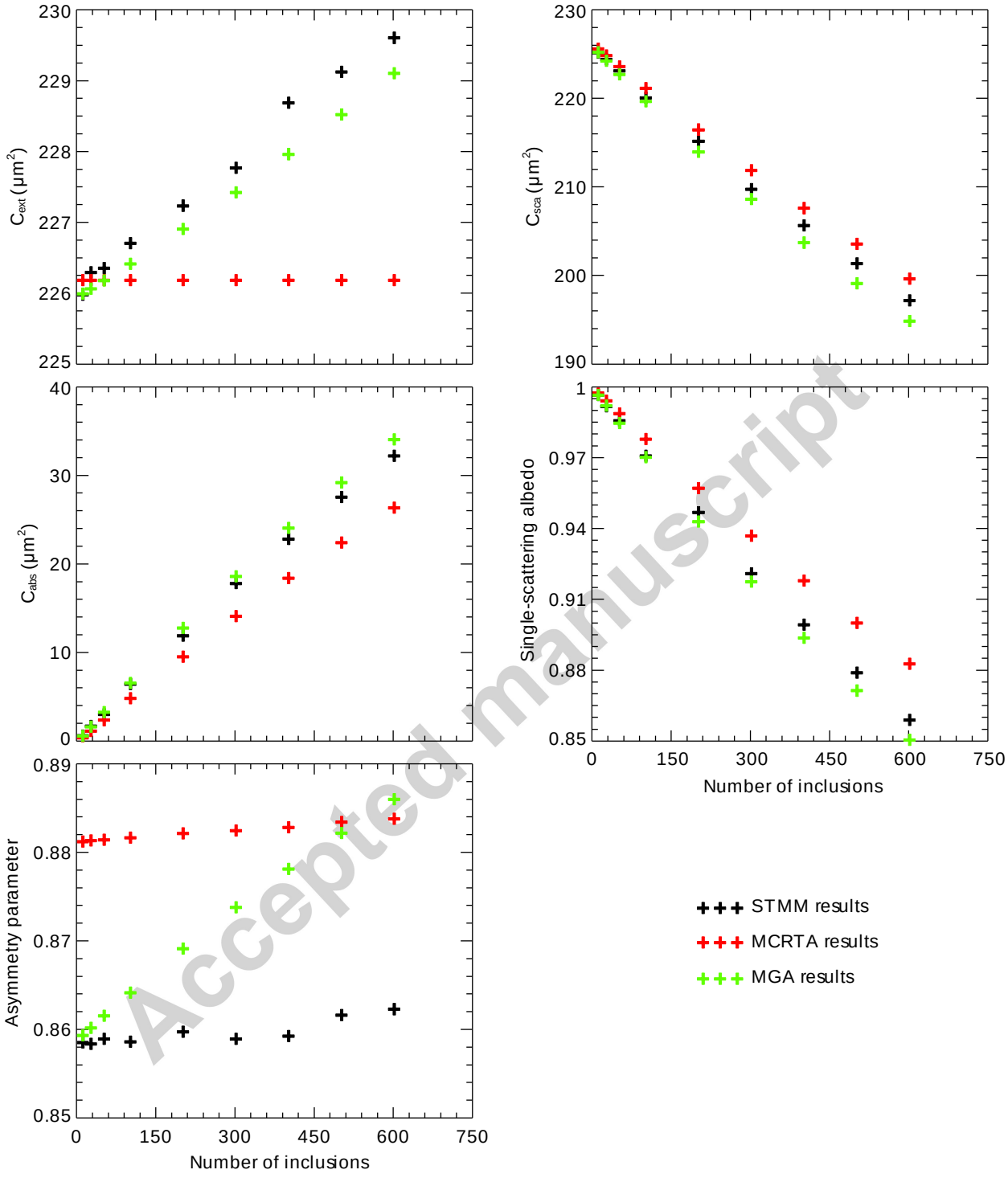

Fig. 5. Comparison of the STMM cross sections, single scattering albedo, and asymmetry parameter with their MCRTA and MGA counterparts.